J|A|C|S ARTICLES

Published on Web 09/02/2010

Electrochemistry and Electrogenerated Chemiluminescence of Dithienylbenzothiadiazole Derivative. Differential Reactivity of Donor and Acceptor Groups and Simulations of Radical Cation−Anion and Dication−Radical Anion Annihilations

Mei Shen,[†] Joaquín Rodríguez-López,[†] Ju Huang,[‡] Quan Liu,[‡] Xu-Hui Zhu,[‡] and Allen J. Bard*[,†]

Center for Electrochemistry, Department of Chemistry and Biochemistry, University of Texas at Austin, 1 University Station, A5300, Austin, Texas 78712-0165, and Institute of Polymer Optoelectronic Materials and Devices, South China University of Technology, Guangzhou 510640, China

Received June 21, 2010; E-mail: ajbard@mail.utexas.edu

Abstract: We report here the electrochemistry and electrogenerated chemiluminescence (ECL) of a red-emitting dithienylbenzothiadiazole-based molecular fluorophore (4,7-bis(4-(4-*sec*-butoxyphenyl)-5-(3,5-di(1-naphthyl)phenyl)thiophen-2-yl)-2,1,3-benzothiadiazole, **1b**). **1b** contains two substituted thiophene groups as strong electron donors at the ends connected directly to a strong electron acceptor, 2,1,3-benzothiadiazole, in the center. Each thiophene moiety is substituted in position 2 by 3,5-di(1-naphthyl)phenyl and in position 3 by 4-*sec*-butoxyphenyl. Cyclic voltammetry of **1b**, with scan rate ranging from 0.05 to 0.75 V/s, shows a single one-electron reduction wave ($E°_{red} = -1.18$ V vs SCE) and two nernstian one-electron oxidation waves ($E°_{1,ox} = 1.01$ V, $E°_{2,ox} = 1.24$ V vs SCE). Reduction of the unsubstituted 2,1,3-benzothiadiazole center shows nernstian behavior with $E°_{red} = -1.56$ V vs SCE. By comparison to a digital simulation, the heterogeneous electron-transfer rate constant for reduction, $k_r° = 1.5 \times 10^{-3}$ cm/s, is significantly smaller than those for the oxidations, $k_o° > 0.1$ cm/s, possibly indicating that the two substituted end groups have a blocking effect on the reduction of the benzothiadiazole center. The ECL spectrum, produced by electron-transfer annihilation of the reduced and oxidized forms, consists of a single peak with maximum emission at about 635 nm, consistent with the fluorescence of the parent molecule. Relative ECL intensities with respect to 9,10-diphenylanthracene are 330% and 470% for the radical anion−cation and radical anion−dication annihilation, respectively. Radical anion ($A^{-\bullet}$)−cation ($A^{+\bullet}$) annihilation produced by potential steps shows symmetric ECL transients during anodic and cathodic pulses, while for anion ($A^{-\bullet}$)−dication ($A^{2+\bullet}$) annihilation, transient ECL shows asymmetry in which the anodic pulse is narrower than the cathodic pulse. Digital simulation of the transient ECL experiments showed that the origin of the observed asymmetry is asymmetry in the amount of generated charges rather than instability of the electrogenerated species.

Introduction

We report the electrochemistry and electrogenerated chemiluminescence (ECL) of a red-fluorescent dithienylbenzothiadiazole derivative (4,7-bis(4-(4-*sec*-butoxyphenyl)-5-(3,5-di(1-naphthyl)phenyl)thiophen-2-yl)-2,1,3-benzothiadiazole, compound **1b**), which is reported to have a high photoluminescence quantum yield (44% of Rhodamine B) and has been studied as a red-emitting electroluminescent and laser dye.[1] Its ECL results from the annihilation reactions between the radical anions and radical cations generated during electrochemical reduction and oxidation. Since **1b** has two oxidation sites, ECL can also be generated through annihilation reactions between the radical anions and dications; thus, we also report on the comparison between simulation and experiment of the transient ECL emission of compound **1b** for the multiply charged radical ion annihilation reactions.

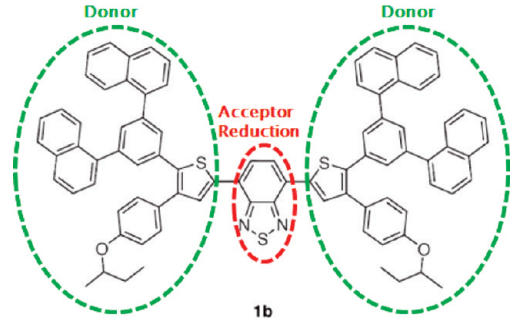

1b

The usual annihilation ECL process of generation of an excited singlet state (S-route) occurs through electron transfer between electrochemically generated species followed by the

[†] University of Texas at Austin.
[‡] South China University of Technology.

(1) Huang, J.; Liu, Q.; Zou, J.-H.; Zhu, X.-H.; Li, A.-Y.; Li, J.-W.; Wu, S.; Peng, J. B.; Cao, Y.; Xia, R. D.; Bradley, D. D. C.; Roncali, J. *Adv. Funct. Mater.* **2009**, *19*, 2978–2986.

emission of light.[2,3] The S-route ECL process can be represented in a general way as shown below:

$$A + e^- \rightarrow A^{-\bullet} \quad \text{(reduction at electrode)} \quad (1)$$

$$D - e^- \rightarrow D^{+\bullet} \quad \text{(oxidation at electrode)} \quad (2)$$

$$A^{-\bullet} + D^{+\bullet} \rightarrow {}^1A^* + D \quad \text{(excited singlet state formation)} \quad (3)$$

$${}^1A^* \rightarrow A + h\nu \quad \text{(light emission)} \quad (4)$$

where A and D are electroactive species and denote acceptor and donor, respectively. A and D can be the same molecule, as in the case of efficient ECL emitter 9,10-diphenylanthracene (DPA).[4,5] They can also be different moieties within the same molecule, as in a donor−acceptor organic molecule. One molecule may have multiple donors or acceptors. A number of donor−acceptor molecules have been the target of ECL studies, for example metal complexes,[6] like the widely used $[Ru(bpy)_3]^{2+}$,[7] in which electrochemical oxidation occurs in the Ru(II) center while three possible reductions can occur in the bipyridine ligands, the emitting state being a metal-to-ligand charge-transfer (MLCT) state.[8] Combination of organic-based D−A motifs allows the design of efficient ECL emitters;[9] high ECL efficiencies have been reported,[10−12] and the possibility of increasing the light yield by using multiple, chemically reversible D or A units has been suggested.[13] Compound **1b** has a 2,1,3-benzothiadiazole moiety as the electron acceptor in the center, connected directly to two donors at the ends. Each donor is a thiophene moiety substituted in position 2 by 3,5-di(1-naphthyl)phenyl and in position 3 by 4-*sec*-butoxyphenyl.

Another interesting aspect of the molecule **1b** is that the acceptor group is "buried" between the two large donor groups. In such structures, heterogeneous electron-transfer kinetics depends on the extent to which the electroactive center is physically removed from the immediate vicinity of the electrode surface, for example, when a molecule is substituted by a long chain or bulky moiety.[14] In compound **1b**, we would expect that the rate constant for reduction, $k_r°$, would be smaller than in the unsubstituted parent 2,1,3-benzothiadiazole molecule. Moreover, one can compare in the same molecule the electron-transfer kinetics for the reduction with those for the oxidation, $k_o°$, of the more exposed donor groups (the thiophene groups). Cyclic voltammetry (CV) studies at different scan rates coupled with digital simulation demonstrate that the electron-transfer rates for the reduction and oxidation processes are indeed different.

Transient ECL generated by alternating potential steps can provide information about the stability of the precursor species (radical anions, radical cations, dications). When the radical ions are generated under mass-transfer-controlled conditions and are stable during a pulse, the ECL emission pulses are of equal height during anodic and cathodic pulses and constant with pulsing. Instability of one of the radical ion species results in unequal heights for the anodic and cathodic pulses and decay of the ECL emission with time.[15] In this paper, we show a comparison between transient ECL generated through radical anion−radical cation and radical anion−dication annihilations; simulations of this transient ECL were carried out. Transient methods for the characterization of ECL, along with a comparison to simulation models, can aid in developing an understanding of the optimum conditions for generating strong and stable ECL emission.[16]

Experimental Section

Materials. Anhydrous acetonitrile (MeCN) and dichloromethane (CH_2Cl_2 or DCM) were obtained from Aldrich (St. Louis, MO) and transferred directly into a helium atmosphere drybox (Vacuum Atmospheres Corp., Hawthorne, CA) without further purification. Electrochemical-grade tetra-*n*-butylammonium hexafluorophosphate ($TBAPF_6$) and 9,10-diphenylanthracene (DPA) were obtained from Fluka and used as received. Tris(2,2′-bipyridine)ruthenium(II) perchlorate (Rubpy) was obtained from GFS Chemicals, Inc. (Powell, OH). Compound **1b** was synthesized as reported recently;[1] characterization details (mass spectrometry, NMR) are contained in the Supporting Information of that paper.

Characterization. The same electrochemical cell was used for both CV and ECL experiments: it consisted of a coiled Pt wire (0.5 mm in diameter) as a counter electrode, a Ag wire (0.5 mm in diameter) as a quasi-reference electrode, and a Pt disk inlaid in glass, bent at a 90° angle (for the disk to face the light detector), as a working electrode. The geometric area of the Pt disk electrode was 0.028 cm^2. After each experiment, the potential of the Ag wire was calibrated with ferrocene (taken as 0.342 V vs SCE).[17] Before each experiment, the working electrode was polished on a felt pad with 0.3 μm alumina (Buehler, Ltd., Lake Bluff, IL) and sonicated in Milli-Q deionized water and then in ethanol. The counter and reference electrodes were cleaned by rinsing and sonicating in acetone, water, and ethanol. Finally, all the electrodes were rinsed with acetone, dried in an oven, and transferred into a glovebox.

Solutions for electrochemical measurements consisted of 0.5 mM **1b** in CH_2Cl_2 as the solvent and 0.1 M $TBAPF_6$ as the supporting electrolyte. All solutions were prepared inside the glovebox. For measurements made outside of the box, the electrochemical cell was closed with a Teflon cap that had a rubber O-ring to form an airtight seal. Stainless steel rods driven through the cap formed

(2) Bard, A. J. In *Electrogenerated Chemiluminescence*; Bard, A. J., Ed.; Marcel Dekker: New York, 2004.
(3) For reviews on ECL, see: (a) Richter, M. M. *Chem. Rev.* **2004**, *104*, 3003–3036. (b) Knight, A. W.; Greenway, G. M. *Analyst* **1994**, *119*, 879–890. (c) Faulkner, L. R.; Bard, A. J. *Electroanalytical Chemistry*; Marcel Dekker: New York, 1977; Vol. 10, p 1. (d) Bard, A. J.; Debad, J. D.; Leland, J. K.; Sigal, G. B.; Wilbur, J. L.; Wohlstadter, J. N. In *Encyclopedia of Analytical Chemistry: Applications, Theory and Instrumentaion*; Meyers, R. A., Ed.; John Wiley & Sons: New York, 2000; Vol. 11, p 9842.
(4) Maloy, J. T. In *Electrogenerated Chemiluminescence*; Bard, A. J., Ed.; Marcel Dekker: New York, 2004; p 159.
(5) Keszthelyi, C. P.; Tokel-Takvoryan, N. E.; Bard, A. J. *Anal. Chem.* **1975**, *47*, 249–256.
(6) Richter, M. M. In *Electrogenerated Chemiluminescence*; Bard, A. J., Ed.; Marcel Dekker: New York, 2004; p 306.
(7) Tokel, N.; Bard, A. J. *J. Am. Chem. Soc.* **1972**, *94*, 2862–2863.
(8) Juris, A.; Balzani, V.; Barigelletti, F.; Campagna, S.; Belser, P.; Von Zelewsky, A. *Coord. Chem. Rev.* **1988**, *84*, 85–277.
(9) Kapturkiewicz, A.; Grabowski, Z. R.; Jasny, J. *J. Electroanal. Chem.* **1990**, *279*, 55–65.
(10) Kapturkiewicz, A.; Herbich, J.; Nowacki, J. *Chem. Phys. Lett.* **1997**, *275*, 355–362.
(11) Lai, R. Y.; Fabrizio, E. F.; Lu, L.; Jenekhe, S. A.; Bard, A. J. *J. Am. Chem. Soc.* **2001**, *123*, 9112–9118.
(12) Lai, R. Y.; Kong, X. X.; Jenekhe, S. A.; Bard, A. J. *J. Am. Chem. Soc.* **2003**, *125*, 12631–12639.
(13) Omer, K. M.; Ku, S.-Y.; Wong, K.-T.; Bard, A. J. *Angew. Chem., Int. Ed.* **2009**, *48*, 9300–9303.
(14) Cardona, C. M.; Mendoza, S.; Kaifer, A. E. *Chem. Soc. Rev.* **2000**, *29*, 37–42.
(15) Cruser, S. A.; Bard, A. J. *J. Am. Chem. Soc.* **1969**, *91*, 267–275.
(16) Forster, R. J.; Bertoncello, P.; Keyes, T. E. *Annu. Rev. Anal. Chem.* **2009**, *2*, 359–385.
(17) Sartin, M. M.; Shu, C. F.; Bard, A. J. *J. Am. Chem. Soc.* **2008**, *130*, 5354–5360.

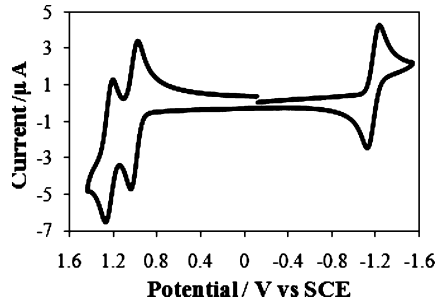

Figure 1. Cyclic voltammogram of 0.5 mM **1b** in dichloromethane with 0.1 M $TBAPF_6$. Scan rate, 100 mV/s; area of electrode, 0.028 cm^2.

Table 1. $E°$, D, and $k°$ for **1b** in Dichloromethane/0.1 M $TBAPF_6$ and 2,1,3-Benzothiadiazole in MeCN/0.1 M $TBAPF_6$

	1b			
	reduction	first oxidation	second oxidation	2,1,3 -benzothiadiazole reduction
$E°$/V vs SCE	−1.18	1.01	1.24	−1.56
10^5 D/cm^2 s^{-1}	1.0(±0.1)	1.1(±0.1)	1.1(±0.1)	3.6(±0.1)
$k°$/cm s^{-1}	1.5×10^{-3}	>0.1	>0.1	>0.1

the electrode connections. Cyclic voltammograms were obtained on a CH Instruments electrochemical workstation (CHI 660, Austin, TX). Digital simulations of CV were performed using Digisim software (Bioanalytical Systems).

Spectroscopic experiments were done in a 1 cm path length quartz cell. Absorbance spectra were obtained on a Milton Roy spectronic 3000 array spectrophotometer. Fluorescence spectra were collected on a QuantaMaster spectrofluorimeter (Photon Technology International, Birmingham, NJ). The excitation source was a 70 W xenon lamp (LPS-220B lamp power supply), and the excitation and emission slits were set to 0.5 mm (2 nm bandwidth).

The ECL spectra were obtained on Princeton SPEC-10 instruments using a charge-coupled device (CCD) camera (Trenton, NJ) cooled to −100 °C, with an Acton SpectraPro-150 monochromator (Acton, MA) as detector. The wavelength scales of the CCD camera and grating system were calibrated using a Hg/Ar pen-ray lamp from Oriel (Stratford, CT). ECL intensity−time curves were collected on an Autolab potentiostat (Eco Chemie, Utrecht, The Netherlands) connected to a photomultiplier tube (PMT, Hamamatsu, R4220p, Japan). The PMT was supplied with −750 V with a Kepco (New York) high-voltage power supply. ECL efficiency was determined with respect to DPA in MeCN and to Rubpy in MeCN by comparing the maximum intensities or emission areas in the ECL spectra, respectively.

Results and Discussion

CV and Digital Simulation. A CV of **1b** in CH_2Cl_2 showed one reduction and two oxidation waves (Figure 1). The standard potentials ($E°$) along with diffusion coefficients (D) and heterogeneous electron-transfer rate constants ($k°$) for **1b** in CH_2Cl_2 and for 2,1,3-benzothiadiazole in MeCN are summarized in Table 1. Overall, the experimental and simulated CV results can be rationalized from the chemical structure of **1b**, which comprises a 2,1,3-benzothiadiazole moiety as the reduction center (A group) and two bulky substituted thiophene end groups as donor groups (D group). After gaining 1e in the center (A group), only a single 1e reduction wave is observed. The two end groups are connected directly to the acceptor center, each capable of losing an electron. The splitting between the oxidation waves of 0.23 V shows that, after the loss of 1e from one end D group, it is more difficult to lose the second electron in the molecule. This indicates that considerable conjugation exists

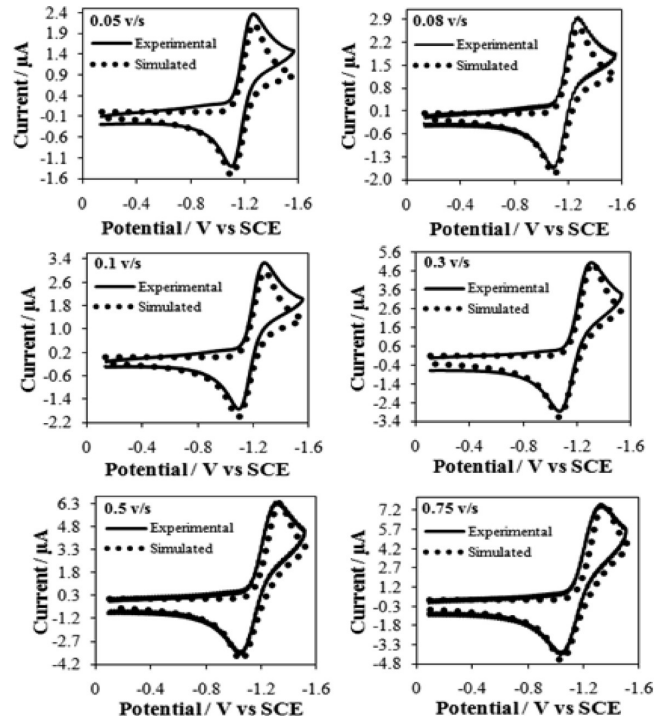

Figure 2. Simulation of 0.5 mM **1b** reduction in dichloromethane at (a) 0.05, (b) 0.08, (c) 0.1, (d) 0.3, (e) 0.5, and (f) 0.75 V/s. Simulation mechanism is one-electron reduction with $D = 1.0 \times 10^{-5}$ cm^2/s, $E°_{red} = -1.18$ V vs SCE, $k° = 1.5 \times 10^{-3}$ cm/s, $\alpha = 0.5$, uncompensated solution resistance $R_u = 1972$ Ω, and double-layer capacitance $C_{dl} = 0.25$ µF.

between these two D groups; CV of other ECL D−A systems have shown that, for molecules with two D groups, the presence of a bulky, nonconjugated spirobifluorene linker between them causes a smaller peak splitting in the 2e oxidation process (∼0.06 V),[17,18] as opposed to a larger splitting observed when the two D groups are connected through a conjugated linker (∼0.18 V).[19] In all of these cases, a doubly charged ion is generated, but the electrostatic repulsive interaction could only account for about a third of what is observed here. Digital simulations of the experimental CVs for the reduction and oxidation are shown in Figures 2 and 3, respectively. These indicate good fits between experimental and simulated CVs for both reduction and oxidation performed at various scan rates from 0.05 to 0.75 V/s. The double-layer capacitance and the uncompensated resistance used in the simulation were measured from a potential step in the region where only double-layer charging occurred, i.e., at 0 V vs SCE. The best fit for the CV simulation suggests a single 1e reduction, with $D = 1.0(\pm0.1) \times 10^{-5}$ cm^2/s and $k° = 1.5 \times 10^{-3}$ cm/s, and two 1e oxidations, with $D = 1.1(\pm0.1) \times 10^{-5}$ cm^2/s and $k° > 0.1$ cm/s.

Heterogeneous Electron Transfer Kinetics. As stated earlier, the structure of **1b** suggests that the reduction of the benzothiadiazole center should be more hindered than that of a free benzothiadiazole molecule and also slower than the oxidation of the external D groups. This expectation is confirmed by the CV results. As shown by the simulation in Figures 2 and 3, a smaller heterogeneous electron-transfer rate constant, $k_r° = 1.5 \times 10^{-3}$ cm/s, was calculated for the reduction occurring in the

(18) Shen, M.; Rodríguez-López, J.; Lee, Y.-T.; Chen, C.-T.; Fan, F.-R. F.; Bard, A. J. *J. Phys. Chem. C* **2010**, *114*, 9772–9780.
(19) Fungo, F.; Wong, K.-T.; Ku, S.-Y.; Hung, Y.-Y.; Bard, A. J. *J. Phys. Chem. B* **2005**, *109*, 3984–3989.

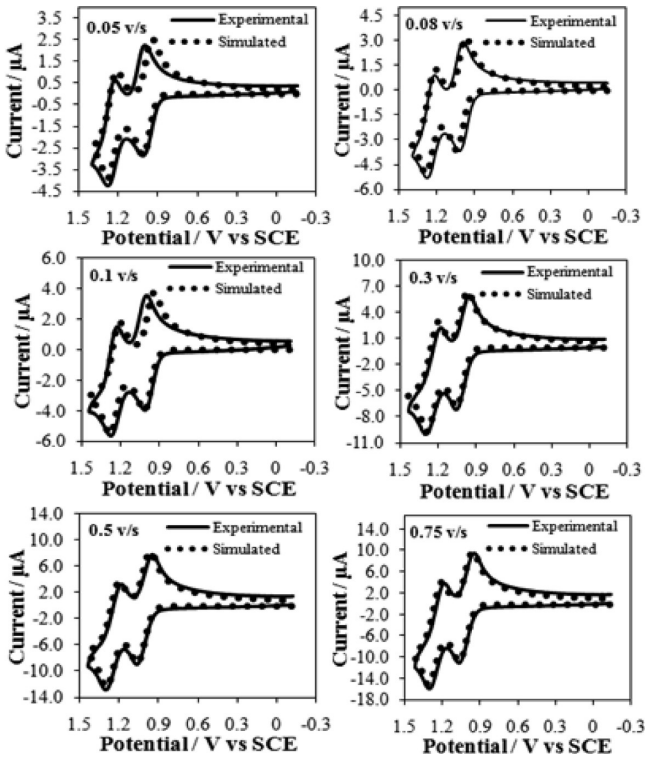

Figure 3. Simulation of 0.5 mM **1b** oxidation in dichloromethane at (a) 0.05, (b) 0.08, (c) 0.1, (d) 0.3, (e) 0.5, and (f) 0.75 V/s. Simulation mechanism is two stepwise 1e oxidations with $D = 1.1 \times 10^{-5}$ cm^2/s, $E^\circ_{1,ox} = 1.01$ V vs SCE, $E^\circ_{2,ox} = 1.24$ V vs SCE, $k^\circ > 0.1$ cm/s, $\alpha = 0.5$, uncompensated solution resistance $R_u = 1972\ \Omega$, and double-layer capacitance $C_{dl} = 0.25\ \mu$F.

acceptor center compared to the oxidations occurring at the two donor ends of the molecule, with $k^\circ > 0.1$ cm/s. Note that the slower measured kinetics for the reduction center cannot be accounted for on the basis of uncompensated resistance, R_u, because (1) this was taken into account in the simulation from the measured R_u and (2) the same value was used for the oxidation and reduction steps. A similar CV study and measurement of the heterogeneous rate constant were carried out for 2,1,3-benzothiadiazole itself (structure shown below).

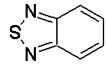

2, 1, 3-Benzothiadiazole

CVs and digital simulations are shown in Figure 4. Because of the poor solubility of this species in CH_2Cl_2, the electrochemical study was carried out in MeCN. In the CV study, only one reduction peak and no oxidation peaks were observed. The CV simulation mechanism assigned a one-electron process for the reduction, with $E^\circ_{red} = -1.56$ V vs SCE, $D = 3.6 \times 10^{-5}$ cm^2/s, and $k^\circ > 0.1$ cm/s. The larger D value is consistent with the smaller size of this molecule compared to **1b**.

The slow electron-transfer rate of the reduction center can be attributed to it being blocked by the two bulky end groups.[14] In fact, when 2,1,3-benzothiadiazole was connected to a small end group (*tert*-butylphenyl), a faster electron-transfer rate for reduction was observed,[20] in contrast to **1b**, where blocking occurs. The distortion of the shape of the reduction CV of **1b** (when compared to the ideal nernstian case) cannot be attributed

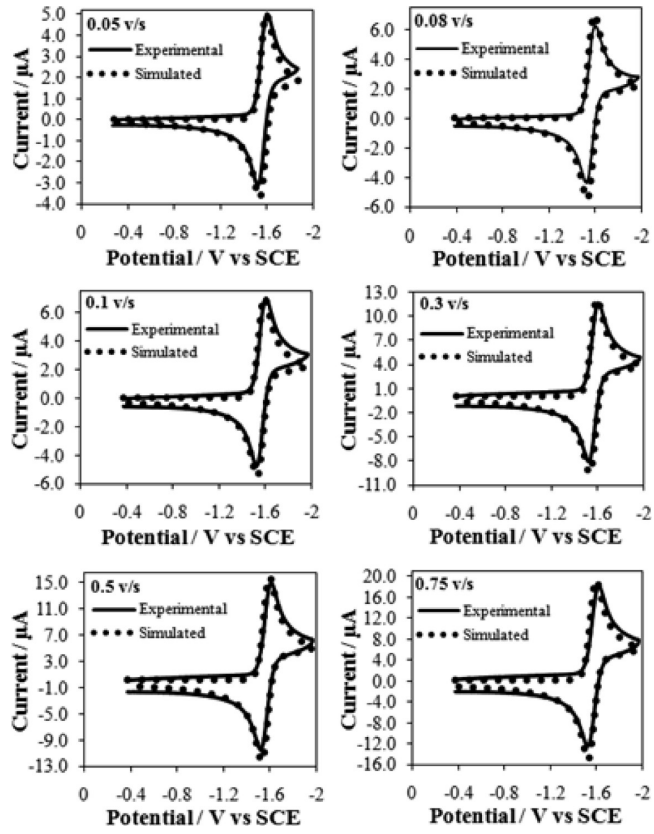

Figure 4. Simulation of 0.5 mM 2,1,3-benzothiadiazole reduction in MeCN at (a) 0.05, (b) 0.08, (c) 0.1, (d) 0.3, (e) 0.5, and (f) 0.75 V/s. Simulation mechanism is one-electron reduction with $D = 3.6 \times 10^{-5}$ cm^2/s, $E^\circ_{red} = -1.56$ V vs SCE, $k^\circ > 0.1$ cm/s, $\alpha = 0.5$, uncompensated solution resistance $R_u = 264\ \Omega$, and double-layer capacitance $C_{dl} = 0.28\ \mu$F.

to a following reaction, as shown by the CV behavior and also by the fact that, as described below, the ECL efficiency is high.[2,3] The slow electron transfer of the A group can be thought of as a forced longer distance electron transfer because of the blockage (a nonadiabatic effect) or the fact that reduction via the accessible thiophene groups would occur at a significantly more negative potential (< -2 V), thus causing a large energy of activation for the reduction. Kojima and Bard[21] studied the heterogeneous electron-transfer kinetics for the reduction of 16 aromatic compounds and found that the total activation energies for reorganization and solvation for all were in the range of 0.1−0.2 eV. Such small activation energies, e.g. for dibenzothiophene, cannot account for the small rate of reduction found here, suggesting that a steric (longer distance) electron transfer is more reasonable.

ECL Studies. The ECL spectra generated by pulsing the electrode potential between the reduction and the two possible oxidations are shown in Figure 5. The ECL generated when stepping into the second oxidation showed a higher intensity for reasons discussed below. Taken together with the results of CV, which showed no indication of decomposition of the radical cation or the dication, and the fact the ECL spectrum is close to the fluorescence spectrum with no additional emission peaks, the precursor stability is high, which is not seen in similar donor−acceptor systems.[17] The relative intensities of **1b** with respect to DPA and Rubpy, both of which are efficient and widely investigated ECL molecules, are shown in Table 2. ECL

(20) Omer, K. M.; Ku, S.-Y.; Wong, K.-T.; Bard, A. J. *J. Am. Chem. Soc.* **2009**, *131*, 10733–10741.

(21) Kojima, H.; Bard, A. J. *J. Am. Chem. Soc.* **1975**, *97*, 6317–6324.

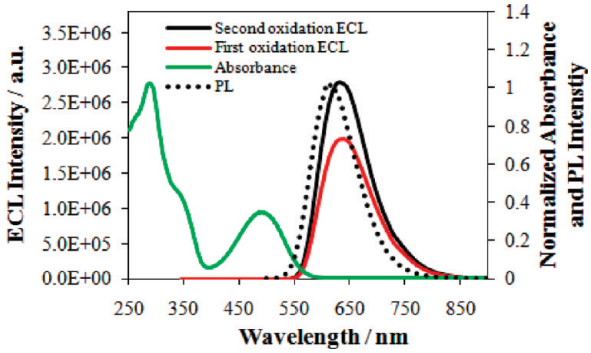

Figure 5. ECL spectra of 0.5 mM **1b** in 0.1 M $TBAPF_6$ in dichloromethane obtained by pulsing between 80 mV past the reduction peak potential and two different anodic potentials, 80 mV past the first oxidation peak potential and 80 mV over the second oxidation peak potential, as well as normalized absorbance and normalized fluorescence or photoluminescence (PL) spectrum of 7 μM **1b** in dichloromethane. ECL spectra were integrated for 30 s using a 0.5 mm slit width. Excitation wavelength for fluorescence emission, 491 nm.

Table 2. Maximum ECL Emission Wavelength λ_{max}^{ECL}, Intensity at λ_{max}^{ECL}, and Relative Intensity with Respect to DPA and Rubpy under Conditions of Figure 5

pulsing potentials	λ_{max}^{ECL} (nm)	$I(\lambda_{max}^{ECL})$ (a.u.)	relative intensity vs DPA (%)[a]	relative intensity vs Rubpy (%)[b]
reduction and first oxidation	637	2.0×10^6	330	81 ± 16
reduction and second oxidation	633	2.8×10^6	470	122 ± 16

[a] Calculated by comparing the $I(\lambda_{max}^{ECL})$ of **1b** with that of DPA in MeCN. [b] Calculated by comparing the $I(\lambda_{max}^{ECL})$ of **1b** with that of Rubpy in MeCN generated by oxidation and first reduction.

intensities of **1b** are stronger than those of DPA when stepping to both the first oxidation and second oxidation, indicating that **1b** is a strong ECL emitter.

There is a 17-nm red shift of the ECL spectrum compared to the fluorescence spectrum, as shown in Figure 5. The compound has a Stokes shift of 120 nm and shows some absorbance within the wavelength range of photoluminescence (PL) and ECL. The concentration of **1b** in the ECL experiments (0.5 mM) was much higher than in the PL experiment (7 μM); thus, absorption of the emitted light in ECL could account for a small inner filter effect that red-shifts the observed ECL emission with respect to that of PL. Systematic errors in the spectroscopy can also account for some of the difference, since the PL and ECL spectra were taken with different instruments and different slit widths; in our experience the accumulated errors typically result in a shift of 10−15 nm. Despite these small discrepancies, the same excited emissive state is probably formed in ECL and in PL.

The energy of the excited singlet state can be estimated from the fluorescence emission maximum by the equation E_s (in eV) $= 1239.81/\lambda$ (in nm),[2] where λ is the wavelength at maximum emission. The calculated excited singlet-state energy is 2.03 eV. The energy of the annihilation reaction, $-\Delta H^\circ = E^\circ_{ox} - E^\circ_{red} - T\Delta S$, based on the difference between the thermodynamic potentials of the first oxidation and the second oxidation and the reduction in the cyclic voltammogram ($E^\circ_{1,ox} - E^\circ_{red} = 2.19$ eV, $E^\circ_{2,ox} - E^\circ_{red} = 2.42$ eV) with an estimated entropy effect (~ 0.1 eV) subtracted out, is about 2.09 and 2.32 eV. The energy of the annihilation reaction (2.09 and 2.32 eV) is greater than the energy needed to directly populate the singlet excited state (2.03 eV), and thus the ECL reaction probably proceeds via the S-route, where the singlet excited state is directly populated upon radical ion annihilation. With a large Stokes shift, a more correct calculation of the energy of the excited singlet-state energy can be estimated by considering the wavelength where the absorbance and emission curves cross; in our case, this would yield an excited singlet state energy of 2.27 eV (at 546 nm), for which our estimated $-\Delta H^\circ = 2.09$ eV for reduction and first oxidation would be insufficient to populate it. Experimentally, we observe that, upon pulsing into the second oxidation process, where $-\Delta H^\circ = 2.32$ eV and the calculated singlet-state energy is higher, the ECL emission profile is maintained, suggesting that, in this excess energy scenario, the same excited state is formed and is thus energy-sufficient, even for the reduction−first oxidation case. Given the apparent high ECL efficiency, even with the uncertainties presented in the calculations, we assign it to an energy-sufficient system.[18]

Experimental and Simulated Transient ECL. In transient ECL experiments, the behavior of the ECL emission is monitored versus time during multiple-potential-step chronoamperometry;[2] this programming alternates the potential of the working electrode between a cathodic potential (radical anion generation) and an anodic potential (radical cation generation). Electrogenerated reactants in excess from pulse $j - 1$ react with freshly electrogenerated reactants generated during pulse j, and so forth. When the radical ions are generated under mass-transfer-controlled conditions and at equal time intervals, i.e., the cathodic pulse is of equal length to the anodic pulse, the ECL emission will show a characteristic decay which is a product of the Cottrell decay along with the consumption of the radical ions by the annihilation reaction. Provided the radical ions are stable, the ECL transient during cathodic and anodic steps should exhibit the same shape, and the intensity of the emission should not decrease with increasing number of steps (after complete development of a quasi-steady-state diffusion layer).[15,22] Much of the early ECL literature included the analysis of these transients for the extraction of kinetic and mechanistic parameters, e.g. through the use of Feldberg plots.[23] However, the complexity of the ECL process has limited its applicability.[2] Our approach in this work is to use transient ECL as evidence of the stability of the radical ions and also to show a particular case in which unequal transients can also be caused by the reactant stoichiometry. Despite the existence of a vast literature on ECL transients and the study of mixed systems,[24] e.g. systems in which D and A in eqs 1 and 2 are located on different molecules and where possibly different stoichiometric amounts of D and A could be used, to the best of our knowledge this case has not been simulated previously and compared to experimental results.[20,25]

a. Experimental ECL Transients. Three kinds of ions can be formed during the reduction and oxidation of **1b**: the radical anion $\mathbf{1b}^{-\bullet}$, the radical cation $\mathbf{1b}^{+\bullet}$, and the dication $\mathbf{1b}^{2+\bullet}$. Figure 6 is a schematic of the polarity and selection of the potential steps for the production of the different ions and shows the results of transient ECL generated by different combinations of these: Figure 6a, in which ECL was generated by radical anion and radical cation annihilation (1-1 case), and Figure 6b,

(22) Bezman, R.; Faulkner, L. R. *J. Am. Chem. Soc.* **1972**, *94*, 3699–3707.
(23) Feldberg, S. W. *J. Am. Chem. Soc.* **1966**, *88*, 390–393.
(24) Forry, S. P.; Wightman, R. M. In *Electrogenerated Chemiluminescence*; Bard, A. J., Ed.; Marcel Dekker: New York, 2004; Chapter 6. Richter, M. M. In *Electrogenerated Chemiluminescence*; Bard, A. J., Ed.; Marcel Dekker: New York, 2004; Chapter 6.
(25) Maloy, J. T. In *Electrogenerated Chemiluminescence*; Bard, A. J., Ed.; Marcel Dekker: New York, 2004; Chapter 3.

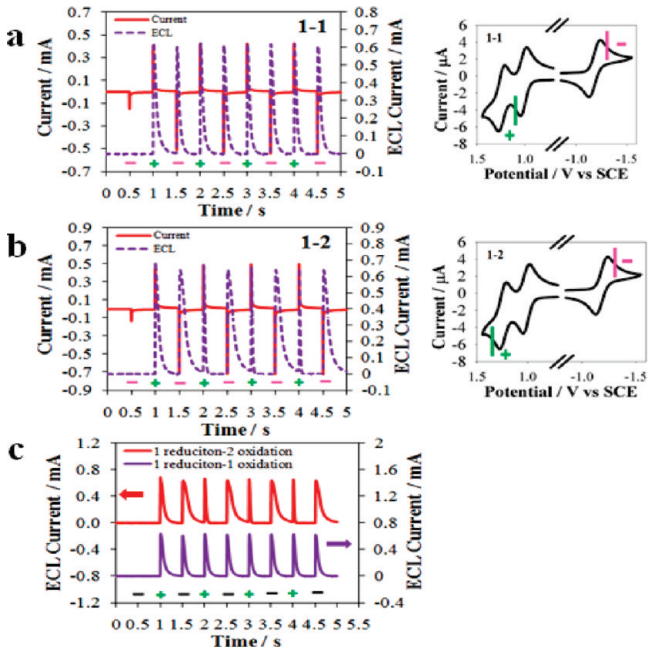

Figure 6. Current (red, solid) and ECL (purple, dotted) transients with 0.5 s pulsing time for 0.5 mM **1b** in dichloromethane (a) pulsed between reduction and first oxidation and (b) pulsed between reduction and second oxidation, and (c) comparison of transient ECL generated through (a) (purple, solid) and (b) (red, solid). Panels on the right show schematically the potentials used and the polarity of the step as indicated in the graphs. + indicates an anodic step or production of radical cations; − indicates a cathodic step or production of radical anions. For the 1-1 case, an oxidation potential of 1.12 V and a reduction potential of −1.32 V were applied; for the 1-2 case, an oxidation potential of 1.36 V and a reduction potential of−1.32 V were applied (vs SCE).

in which ECL was generated by radical anion and dication annihilation (1-2 case). Both cases show that the ECL responses are fairly stable, in that the transient response does not decrease with the number of steps, thus indicating, as grasped from the chemical reversibility in the CV shown in Figure 1, no evident loss of **1b** or its electrochemically reduced/oxidized species due to chemical decomposition into other products. This feature is characteristic of strongly emitting ECL systems.

As shown in Figure 6a, the ECL transient generated by radical anion−cation annihilation exhibits a symmetrical response during the anodic and cathodic pulses; in Figure 6b, however, where ECL is generated by anion−dication annihilation, a broader ECL signal was obtained during the cathodic pulse compared to the anodic pulse. This can be more clearly observed in the comparison made in Figure 6c between the two experimental cases. A possible misinterpretation of the shape of the transients in Figure 6b without taking into account the effects of the stoichiometry of the reaction could suggest that the radical anion is chemically unstable, so that, upon anodic stepping (production of dications), the ECL intensity decays faster in time as a consequence of the decomposition of the anions.[15] This explanation is contrary to the stability observed in the transients of Figure 6a for the 1-1 case, and also because the overall ECL emission is increased when comparing the 1-2 case with respect to the 1-1 case; furthermore, the CV of **1b** does not suggest any chemical instability. The difference in the shape of the 1-2 case with respect to the 1-1 case in Figure 6c can be better explained by the following arguments that take into account the stoichiometry of the reactants. In the first cathodic pulse ($t = 0.5$ s, j), $\mathbf{1b}^{-\bullet}$ is produced; since no radical cations are initially present in the system, there is no ECL emission at $t = 0.5$ s. In the following first anodic pulse ($t = 1$ s, $j + 1$), $\mathbf{1b}^{+\bullet}$ or $\mathbf{1b}^{2+\bullet}$ (for the 1-2 case) is freshly produced and reacts with $\mathbf{1b}^{-\bullet}$ produced in step j and ECL emission is observed; $\mathbf{1b}^{-\bullet}$ is the limiting species in both cases, so the same ECL emission profile is produced for the first anodic pulse as evidenced in Figure 6c at $t = 1$s. Since in the 1-2 case a larger amount of charge is injected for the generation of $\mathbf{1b}^{2+\bullet}$ at pulse $j + 1$ compared to the 1-1 case, more radical cations are left to react with $\mathbf{1b}^{-\bullet}$ for the following cathodic pulse ($t = 1.5$ s, $j + 2$), thus a broader peak is observed for the 1-2 case; after the cathodic pulse at 1.5 s, less $\mathbf{1b}^{-\bullet}$ is left for the following anodic pulse ($t = 2$ s, $j + 3$) as a consequence of a larger amount of radical cations having been consumed during pulse $j + 2$, thus a narrower ECL signal is seen in pulse j+3 compared to the 1-1 case; the following pulses can be described by these same arguments. To understand and quantify the observed differences, simulation of transient ECL was performed, and the results are shown below.

b. Digital Simulation of Transient ECL. Electrochemical and ECL digital simulations were carried out using the COMSOL Multiphysics software v.3.2 which uses a finite element method (FEM) to treat diffusion and reaction kinetics. The problem was solved in the transient mode, and a 1D approach was used to model planar diffusion to the electrode. While the use of an exponentially expanding grid has been criticized for ECL simulations using the finite difference method,[26] it did provide the necessary stability and memory efficiency required to treat the coupled homogeneous and heterogeneous electrochemical conditions in this FEM simulation.

Figure 7 shows a summary of the simulation model, where the required reactions for the ECL process (panel A) have been expanded from those shown in eqs 1−4 to account also for the possibility of electrogeneration of a dication in addition to the radical cation and radical anion, the annihilation reaction between a dication and a radical anion, and the nontrivial oxidation of the parent molecule by the dication (comproportionation). Panel B shows the discretization of the simulation space; this was performed by using an exponentially expanding grid with a base box length of Δx_0 =15 nm and an element growth factor of 1.2 ($\beta = 0.2$, where $\Delta x_k = \Delta x_0\, e^{k\beta}$, Δx_k being the size of simulation element k). For a simple potential step at a diffusion-limited potential and following Cottrell behavior, the size of the simulation space should accommodate at least 6−7 times the extension of the diffusion layer δ, where $\delta \approx (2Dt)^{1/2}$, D being the diffusion coefficient of the species and t the length of the potential step. While in transient ECL the potential is being stepped to different values, δ can be safely approximated using the total time of the experiment. For our typical simulations and experiments, $t \approx 10$ s and $D = 1 \times 10^{-5}$ cm^2/s, as explained earlier in the text, so $7\delta \approx 989\ \mu$m; as shown in Figure 7B, we decided to use a simulation space 1 mm in length (55 simulation elements), where the region closest to the electrode is meshed the finest.

The potential versus time programming used for the electrode boundary is shown in Figure 7C; the simulated stepping was accomplished by setting a time-dependent sine wave as the argument of a step function that alternated between an oxidizing and a reductive potential, E^+ and E^-, respectively, thus resulting in a square wave with a potential step length of 0.5 s, as described experimentally in Figure 6. The use of Butler−Volmer (B-V) kinetics to describe the flux of electroactive species with

(26) Feldberg, S. W. *J. Elecroanal. Chem.* **1981**, *127*, 1–10.

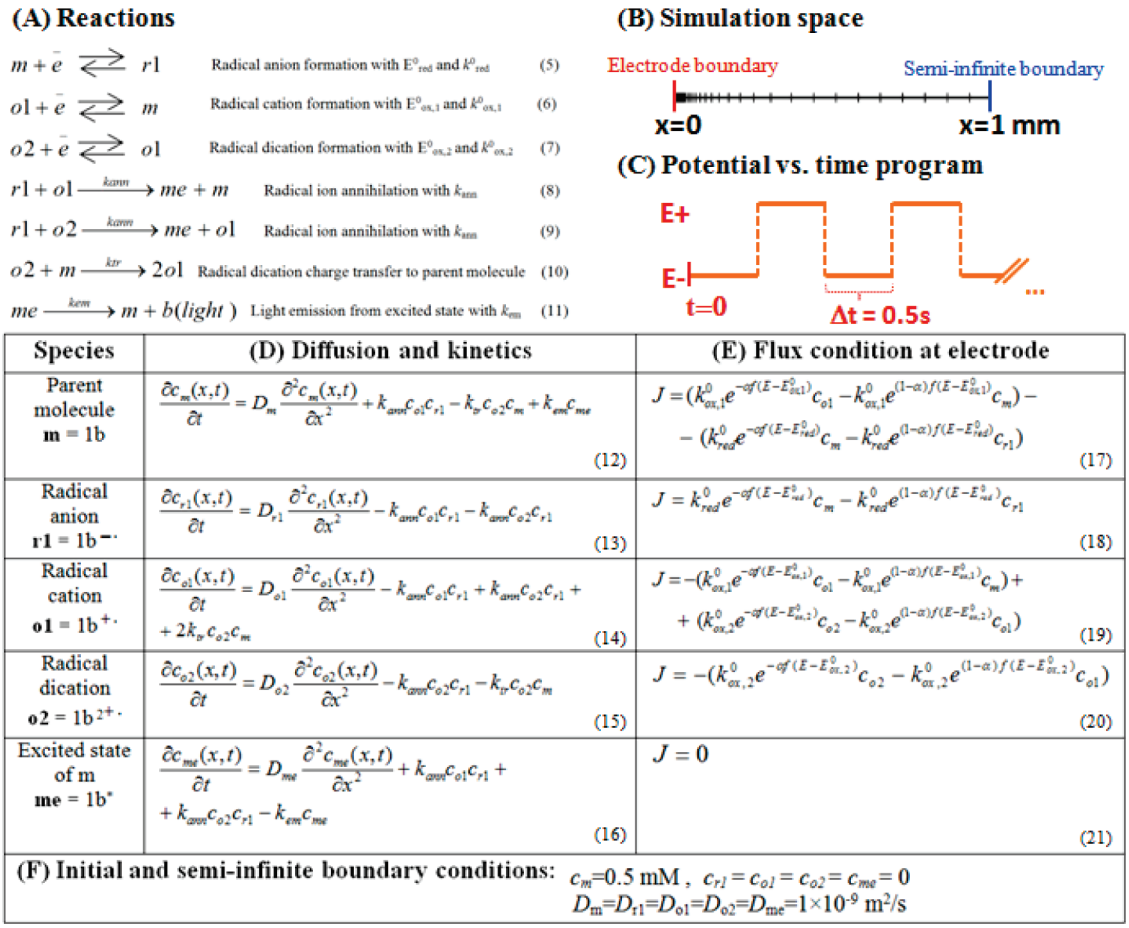

Figure 7. Summary of simulation model used for transient ECL. (A) Chemical and electrochemical reactions used, eqs 5−11. (B) 1D simulation space showing the spatial simulation elements and the relevant boundaries. (C) Programming used for the electrode potential vs time; (D) Coupled diffusion and kinetics used in the simulation space for each species, eqs 12−16. (E) Butler−Volmer expressions for the flux to the electrode boundary for each species, eqs 17−21. (F) Initial and semi-infinite boundary conditions used.

respect to the electrode boundary allows relating the potential programming to the operation of the electrode (eqs 17−21). As well, the use of Fick's second law of diffusion, including reaction kinetics, allows the description of the following chemical reaction mechanisms necessary for the ECL process in the simulated space (eqs 12−16). The respective equations for these two processes are shown in Figure 7D for each participating species; species that can either be both reduced and oxidized, e.g. the parent molecule and the radical cation, required the use of more than one B-V expression to be described. Figure 7F also shows the initial and semi-infinite boundary conditions, which indicate that only the parent molecule is present at the beginning of the experiment and in the bulk of the solution.

For the evaluation of the model equations in Figure 7, all second-order kinetics were assumed to be fast and to proceed close to diffusion limitation, such that $k_{ann} = k_{tr} = 1 \times 10^9$ M^{-1} s^{-1}, and the radiative decay of the excited state of the parent molecule was assumed to have a lifetime of 1 ns, such that $k_{em} = 1 \times 10^9$ s^{-1}, a typical value for fluorescence emission.[27] For the evaluation of the B-V kinetics, we assumed that the transfer coefficient $\alpha = 0.5$, $f = 38.94$ V^{-1} (where $f = F/RT$, with the Faraday constant $F = 96\,485$ C/mol, the gas constant $R = 8.314$ J/mol, and the temperature $T = 298$ K), and the standard rate constant k° for the two reversible oxidations $k^\circ_{ox,1} = k^\circ_{ox,2} = 10$ cm/s and for the reduction $k^\circ_{red} = 1.5 \times 10^{-3}$ cm/s, in accordance with the text. For the evaluation of the potential expressions in the B-V model, a simplification was used in order to avoid very large numbers in the evaluation of the exponentials, which led to instabilities in the numerical evaluation. Such simplification involved decreasing the potential gap between $E^\circ_{ox,1}$ (first oxidation) and E°_{red} (first reduction) to manageable values without affecting the accuracy of the results; i.e., the experimental energetic gap of 2.19 V between $E^\circ_{ox,1}$ and E°_{red} was reduced to 0.6 V. The used standard potentials used were $E^\circ_{ox,1} = 0.3$ V, $E^\circ_{ox,2} = 0.53$ V, and $E^\circ_{red} = -0.3$ V, and the selected stepping potentials, which operate under diffusion-limited conditions, were $E^+ = 0.36$ V and $E^+ = 0.59$ V for the first and second oxidation processes, respectively, and $E^- = -0.36$ V for the reduction process. The values chosen for the stepping and standard potentials for the oxidation reactions at the electrode are in accordance with the potential separation between the first and second oxidations observed experimentally in order to accurately compare simulation and experiment.

The simulated ECL signal was obtained by two approaches, the first one by integrating the rate of emission of the excited state, eq 11 in Figure 7A, across the simulation space at specified intervals (time stepping = 1 ms) and the second one by modeling the emitted light (species *b* in Figure 7A, eq 11) as a pseudoparticle with extremely high diffusion coefficient (e.g.,

(27) Lakowicz, J. R. *Principles of Fluorescence Spectroscopy*, 3rd ed.; Springer Science + Business Media: New York, 2006.

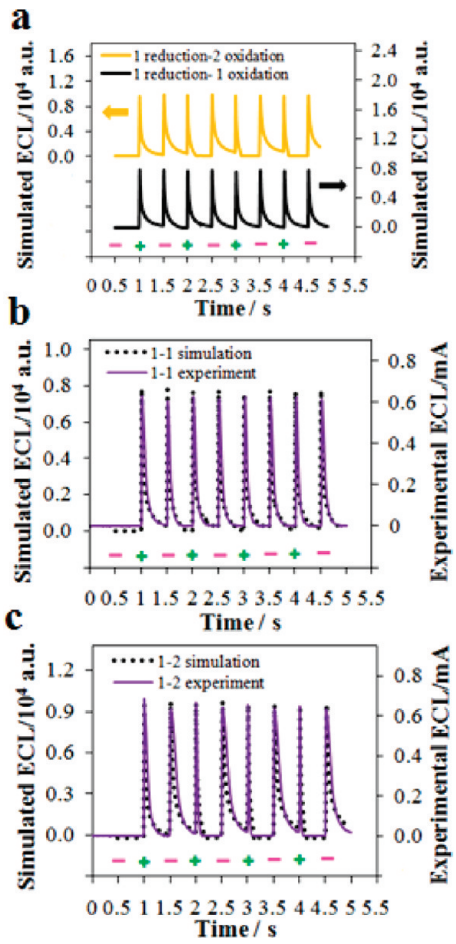

Figure 8. Comparison between simulated and experimental results for transient ECL: (a) simulated transients for the 1-1 (black) and 1-2 (yellow) cases, where − and + signs indicate cathodic and anodic stepping respectively, and all other conditions are as explained in the text; (b) comparison for the 1-1 case between simulation (dotted) and experimental (continuous) transients on the same scale; (c) same as (b) but for the 1-2 case. Simulated transients neglect the first 5 ms of each step.

$D = 10^7$ cm^2/s), and integrating its flux at the electrode boundary to obtain a "photonic current".[25] While the units of the ECL signal are arbitrary (i.e., do not include effects from the quantum efficiency of emission, geometry of photon collection, or response of the detector), the relative intensities and shape of the response were consistent upon comparison of both transients (e.g., by overlapping them on the same scale). Comparison of the simulated and experimental results was done in the same fashion and is shown in Figure 8 for the two cases of interest, i.e. the reaction of the radical anion generated at E^- and either the radical cation (1-1 case) or dication (1-2 case) generated at E^+.

Figure 8a shows the comparison of the two simulation results, 1-1 case and 1-2 case, and Figure 8b,c shows the comparisons of the corresponding experimental and simulated results. Qualitatively there is a very good agreement between the experimental and simulated results; the simulation effectively recreates the following features: (1) There is a predicted difference in the shape of the ECL transients when comparing the 1-1 case to the 1-2 case; that is, upon changing the stoichiometry of the problem without the need to include other effects such as instability of the radical ions. (2) The relative widths and intensities of the curves agree well with the experimental ones, the simulation predicting in the 1-2 case narrower transients for the anodic pulses and wider ones for the cathodic pulses when compared to the 1-1 case. (3) The first transient, i.e. $t = 1$ s, shows no difference between the 1-1 and 1-2 cases due to the role of $\mathbf{1b}^{-\bullet}$ as the limiting reactant, as explained in the discussion of Figure 6. The fit is satisfactory, considering the simplifications of the mechanism used (Figure 7).

Table 3. Quantitative Comparison of Experimental and Simulated Results Obtained by Numerical Integration of ECL Transients

relation	species	predicted	experimental/detector[b]
T_S:$T_{T(1:1)}$	**1b**	0.5	0.47 ± 0.03 PMT
T_L:$T_{T(1:1)}$	**1b**	0.5	0.53 ± 0.017 PMT
T_S:$T_{T(1:2)}$	**1b**	0.25	0.17 ± 0.04 PMT
T_L:$T_{T(1:2)}$	**1b**	0.75	0.83 ± 0.07 PMT
$T_{T(1:1)}$:$T_{T(1:2)}$	**1b**	1.43	1.3 ± 0.10 PMT
			1.4 ± 0.3 CCD
$T_{T(1:1)}$:$T_{T(1:2)}$	Rubpy	1.43	1.6 ± 0.15 CCD
$T_{T(1:1)}$:$T_{T(1:1)}$	Rubpy:**1b**	N/A	1.1 ± 0.2 CCD
$T_{T(1:2)}$:$T_{T(1:2)}$	Rubpy:**1b**	N/A	1.2 ± 0.14 CCD

[a] Nomenclature: $T_{T(x:y)}$, total transient for one cycle with stoichiometry x:y; T_L, large transient component; T_S, small transient component. [b] PMT and CCD indicate whether the detector of ECL measurement is a photomultiplier tube or charge coupled device respectively as described in the text. Standard deviations were obtained from three relevant measurements.

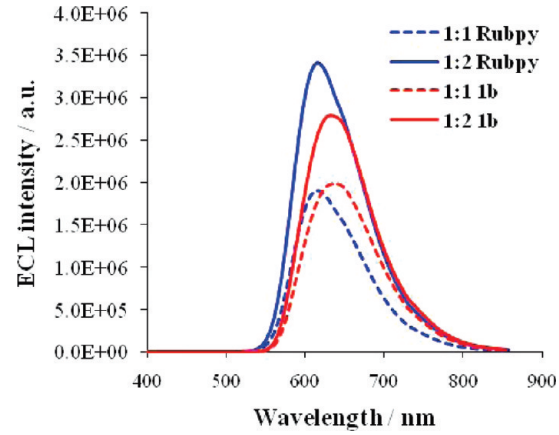

Figure 9. Comparison of ECL emission spectra for the 1-1 cases (dotted lines) and 1-2 cases (continuous lines) for Rubpy (blue) and **1b** (red); 0.5 mM Rubpy in MeCN and 0.5 mM **1b** in CH_2Cl_2 with 0.1 M $TBAPF_6$ as supporting electrolyte. Area of electrode, 0.028 cm^2; step time, 0.1 s; slit width, 0.5 mm; integration time, 30 s. For 1-1 Rubpy, the spectrum was generated by pulsing between 1.28 V (80 mV over oxidation peak potential) and −1.53 V (50 mV over first reduction peak potential); for 1-2 Rubpy, the spectrum was generated by pulsing between 1.28 V (80 mV over oxidation peak potential) and −1.73 V (50 mV over second reduction peak potential) versus Ag electrode.

The goodness of the fit between the experimental and simulated results for **1b** was further tested quantitatively; this can be done by comparing the relative integrated intensities of both experimental and simulated transients. Table 3 shows the results for relevant comparisons of the features exhibited by the ECL transients of **1b** and ruthenium tris-bipyridine (Rubpy), an ECL standard with a similar emission profile (shown in Figure 9) and a high ECL emission quantum yield. Rubpy is also able to generate a 2e reduced state that produces stable annihilation ECL. Table 3 shows that, upon comparison of the different possible transients to the total emission in one cycle for **1b**, the results are comparable to the predicted ones, within the standard deviation of the measurements, for both the 1-1 case (T_S:$T_{T(1:1)}$ and T_L:$T_{T(1:1)}$) and the 1-2 case (T_S:$T_{T(1:2)}$ and T_L:$T_{T(1:2)}$).

The total emission intensity of the 1-1 case with respect to the 1-2 case ($T_{T(1:1)}$:$T_{T(1:2)}$) is a useful parameter; a naive expectation might be that the system would show twice the ECL emission for the 1-2 case. However, the combined effects of ECL annihilation and diffusion into the bulk of the solution and electrochemical deactivation of ions must be taken into account (e.g., $\mathbf{1b}^{2+\bullet}$ is prone both to react with $\mathbf{1b}^{-\bullet}$ and to get reduced at the electrode during a cathodic pulse). The simulation predicts 1.43 times more total light in the 1-2 case with respect to the 1-1 case, which agrees with the experiment with **1b** and was proved by the use of two different signal transducers. Furthermore, this figure is also confirmed within reasonable accuracy in the case of Rubpy. The relationships presented in Table 3 are directly comparable to the experiments shown in this study. Nonetheless, simulation of the cases where the diffusion coefficient of the species was increased or decreased by 1 order of magnitude (e.g., 1×10^{-4} cm^2/s > D > 1×10^{-6} cm^2/s) and in which the step time was changed in the same fashion (e.g., 0.05 s > t > 5 s) revealed no changes in this relative quantification. A final quantitative measurement displayed in Table 3 and shown experimentally in Figure 9 is the comparison of the total intensity of emission of **1b** in comparison to Rubpy under similar conditions. Rubpy is a good standard for comparison to **1b** because of their similar emission characteristics, as shown in Figure 9. Our results indicate that the emission produced by **1b** is of comparable intensity to that produced by Rubpy, which complements also the data shown in Table 2 for DPA and **1b**.

The simulation presented for the 1-2 case can also be placed in the context of other stoichiometric relationships. Figure 10a shows the simulated results for the ECL transients when one of the radical ions is produced in excess with respect to the other. The trend observed for the 1-2 case is followed; upon increasing the equivalents of one component with respect to the other, the transients show the narrowing of one part of the ECL emission and the broadening of the other. We found a linear relationship between the total emission intensity of ECL in one cycle compared to the 1-1 case with respect to the excess of equivalents, as shown in Figure 10b, although as already mentioned the slope is not equal to 1 due to a contribution of kinetic, diffusive, and electrochemical factors. Our group is currently involved in the search and study of D−A systems that can fulfill these predictions.

Conclusions

We have studied the ECL of a red, highly fluorescent molecular dye and presented the digital simulation of transient ECL. The molecule can produce strong ECL without a co-reactant. The ECL intensity of this compound is higher than that of the well-known ECL emitter DPA. ECL generated by anion−dication annihilation is stronger than that of anion−cation annihilation. Transient ECL responses corresponding to anodic and cathodic pulses have equal height and are stable with increasing pulses. The radical anion, cation, and dications of the dye were stable. Transient ECL was successfully simulated using a finite element package. The energies of both of the annihilation reactions are sufficiently high that direct generation of the singlet excited state, with the corresponding ECL emission, is probable. Electron transfer to a buried acceptor site is slower than oxidation of the more accessible donor sites in the same molecule.

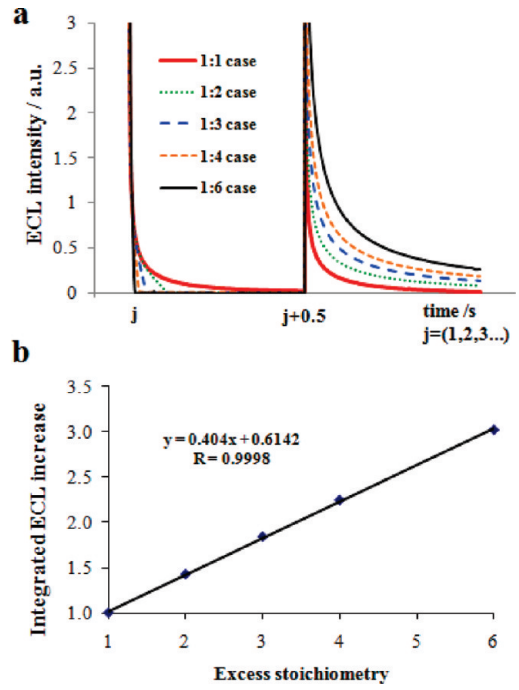

Figure 10. Simulated ECL transients for different stoichiometric cases and quantification of the increase in their ECL intensity compared to the 1-1 case: (a) shape of ECL transients for a 0.5 train of pulses; (b) linear plot of the increase of total ECL intensity in one cycle (i.e., both cathodic and anodic pulses) with respect to the 1-1 symmetrical case versus the excess stoichiometry (e.g., for the 1-2 case, $x = 2$).

Acknowledgment. We thank Roche Diagnostics, the National Science Foundation (CHE 0808927), and the Robert A. Welch Foundation (F-0021) for financial support of this research and Chongyang Liu for helpful discussions. J.R.-L. thanks Eli Lilly & Co. for an American Chemical Society Division of Analytical Chemistry fellowship and also thanks the Secretaria de Educacion Publica of Mexico and the Mexican Government for scholarship support. X.-H.Z. is deeply grateful for the financial support from NNSF, MOE, and MOST of China (Grant Nos. 50603006, NCET-2006-0750, and 2009CB930604).

Note Added after ASAP Publication. Figure 3 is incorrect in the version published ASAP September 2, 2010; the correct version reposted September 22, 2010.

JA105282U